Materials Today Bio 31 (2025) 101620

Contents lists available at ScienceDirect

Materials Today Bio

journal homepage: www.journals.elsevier.com/materials-today-bio

Ultrasound-responsive engineered bacteria mediated specific controlled expression of catalase and efficient radiotherapy

Zichao Liu [a,b,d,1], Lingling Lei [a,b,1], Zenan Zhang [a,b,d], Meng Du [a,b,*], Zhiyi Chen [a,b,c,**]

[a] Key Laboratory of Medical Imaging Precision Theranostics and Radiation Protection, College of Hunan Province, The Affiliated Changsha Central Hospital, Hengyang Medical School, University of South China, Changsha, China
[b] Institute of Medical Imaging, Hengyang Medical School, University of South China, Hengyang, China
[c] Department of Medical Imaging, The Affiliated Changsha Central Hospital, Hengyang Medical School, University of South China, Changsha, China
[d] The Seventh Affiliated Hospital, Hunan Veterans Administration Hospital, Hengyang Medical School, University of South China, Changsha, Hunan, China

ARTICLE INFO

Keywords:
Hypoxia relief
Sensitization
Catalase
Ultrasound
Engineering bacteria
Breast cancer

ABSTRACT

The limited efficacy of radiotherapy (RT) in breast cancer is intricately linked to the hypoxic tumor microenvironment. Delivering catalase (CAT) to decompose hydrogen peroxide (H_2O_2) into oxygen is a promising strategy to address this. However, challenges such as low transport efficiency, accumulation in normal organs, and lack of spatiotemporal control hinder its clinical application. To address this, we developed an innovative ultrasound-responsive engineered bacteria-based CAT delivery system (UEB), which effectively overcomes these challenges by targeting tumors, ensuring efficient CAT expression, and providing precise spatiotemporal control over H_2O_2 decomposition. When subjected to ultrasound irradiation, the decomposition of H_2O_2 and the production of oxygen by UEB increased threefold, demonstrating excellent capability in alleviating hypoxia. CAT accumulation in normal organs was minimized through this ultrasound-responsive delivery strategy. Moreover, these engineered bacteria enhance reactive oxygen species (ROS) generation, improving RT outcomes and significantly inhibiting tumor growth, resulting in a 10-fold tumor size reduction. This study demonstrates a promising strategy for the specific, controlled expression of CAT by the application of ultrasound-responsive engineered bacteria to enhance the efficacy of tumor radiotherapy.

1. Introduction

As the most frequently diagnosed cancer among women worldwide, Breast cancer severely threatens women's health and lives [1]. Radiotherapy (RT) is a crucial therapeutic approach for managing breast cancer, utilizing high doses of ionizing radiation to induce the formation of reactive oxygen species (ROS) and DNA damage, ultimately eradicating cancer cells and inhibiting tumor growth [2–4]. However, the hypoxic tumor microenvironment (TME) limits the efficacy of RT due to insufficient ROS production [5,6]. Increasing oxygen concentration to alleviate tumor hypoxia is vital to enhance radiotherapy efficiency [7]. Common methods to alleviate tumor hypoxia include external oxygen delivery [8], in situ oxygen production [9], and enhancing blood flow within tumor tissues to elevate oxygen levels in solid tumors [10]. Given the abundant hydrogen peroxide (H_2O_2) present in tumor tissues, delivering "enzymes" such as catalase (CAT) to decompose excess H_2O_2 into oxygen is an attractive approach [11,12].

The concentration of CAT is important for alleviating hypoxia tumor microenvironment. Various systems have been developed to improve CAT accumulation in tumors [13,14]. With the advancement of synthetic biology, strategies that integrate bacterial systems with genetic modification have gained considerable attention. Bacteria can actively target hypoxic tumor microenvironments and express functional proteins through prokaryotic expression vectors, enhancing protein delivery efficiency [15–17]. It has demonstrated that the expression of bacteria successfully resulted in an increased concentration of proteases within the tumor [18].

While a promising strategy for tumor-targeted delivery was

* Corresponding author. 161 Shaoshan South Road, Changsha, China.
** Corresponding author. 161 Shaoshan South Road, Changsha, China.
E-mail addresses: dumeng_work@126.com (M. Du), zhiyi_chen@usc.edu.cn (Z. Chen).
[1] These authors have contributed equally to this work and share the first authorship.

https://doi.org/10.1016/j.mtbio.2025.101620
Received 30 December 2024; Received in revised form 17 February 2025; Accepted 26 February 2025
Available online 27 February 2025

presented through the application of bacteria to express exogenous proteins, considerations regarding the specificity and efficiency of protein expression are paramount. The H_2O_2 balance may be disrupted due to the accumulation of CAT in normal tissues, adversely affecting antimicrobial defense, apoptosis, aging, inflammation, tumorigenesis, and overall health with potential oxidative stress imbalances [19]. Besides, metabolic burden, which significantly has a negative impact on bacterial viability and reduces protein synthesis efficiency, thereby limiting the therapeutic effectiveness of bacterial therapies for tumors, happens when bacteria express exogenous genes continually [20]. To address these challenges, the application of inducible plasmids for engineering bacteria enables the specific expression of CAT at tumor sites while preserving bacterial viability and protein synthesis efficiency. It has demonstrated the utility of inducible plasmid systems for modulating bacterial function and controlling protein expression [21,22]. Among the various techniques available, ultrasound stands out for its non-invasive, safe properties and its ability to penetrate tissues. Notably, the ability of ultrasound-excited wavefronts to focus on deep tumors and generate thermal effects allowed for precise and localized control of protein expression through temperature-regulated promoter elements [16,23].

In our preliminary studies, it was confirmed that the expression of interferon-γ in engineered bacteria can be effectively regulated by US, which leads to enhanced spatiotemporal control of protein expression and yields promising therapeutic effects against tumors. Additionally, the accumulation of this bacterium in tumor tissues and major organs of mice over time was validated, demonstrating its specific active targeting capability toward tumors and prolonged tumors retention [24]. In this study, an ultrasound-responsive engineered bacterium (UEB) was redeveloped based on previous bacterial research, which can spatiotemporally control the expression of CAT through focused ultrasound-induced thermotherapy. In this system, CAT genes are inserted into the multiple cloning sites under the tandem PL and PR promoters and subsequently transformed into E. coli MG1655, UEB can accumulate in hypoxic and necrotic tumor regions (Fig. 1). Upon delivery to the tumor, CAT gene expression was triggered by focused ultrasound irradiation, facilitating the decomposition of H_2O_2 into oxygen, thereby relieving hypoxic conditions in the TME. The production of CAT resulted in an enhancement of cancer cell apoptosis by RT and significant inhabitation of tumor growth. Notably, compared to chemical induction, specific CAT accumulation within the tumor was achieved through the UEB combined with focused ultrasound. Thus, a high spatiotemporal control and effective CAT delivery strategy was presented to enhance radiotherapy efficiency through ultrasound-responsive engineered bacteria.

2. Methods and materials

2.1. Cell culture

4T1 mouse breast cancer cells (ATCC) were cultured in DMEM with 5 % FBS and 1 % penicillin-streptomycin at 37 °C under normoxic (21 % O_2, 5 % CO_2) or hypoxic (2 % O_2, 93 % N_2, 5 % CO_2) conditions. Cell digestion was performed using 0.25 % EDTA trypsin (Gibco, America).

2.2. CAT plasmid and preparation of UEB and IEB

The CAT gene sequence was obtained from GenBank, and the thermosensitive plasmid pBV220-CAT was synthesized by Sangon Biotech (China). E. coli DH5α was transformed with the plasmid, and successful construction was verified by enzyme digestion. The pBV220-CAT plasmid was then introduced into E. coli MG1655 (MIAOLING BIOLOGY, China) to create the UEB strain. UEB colonies were grown on ampicillin plates, amplified overnight at 30 °C, and inoculated into LB medium. The OD600 reached 0.4–0.6 before further use. Another bacterium, IEB, was selected, and its plasmid pET-28a-CAT was synthesized

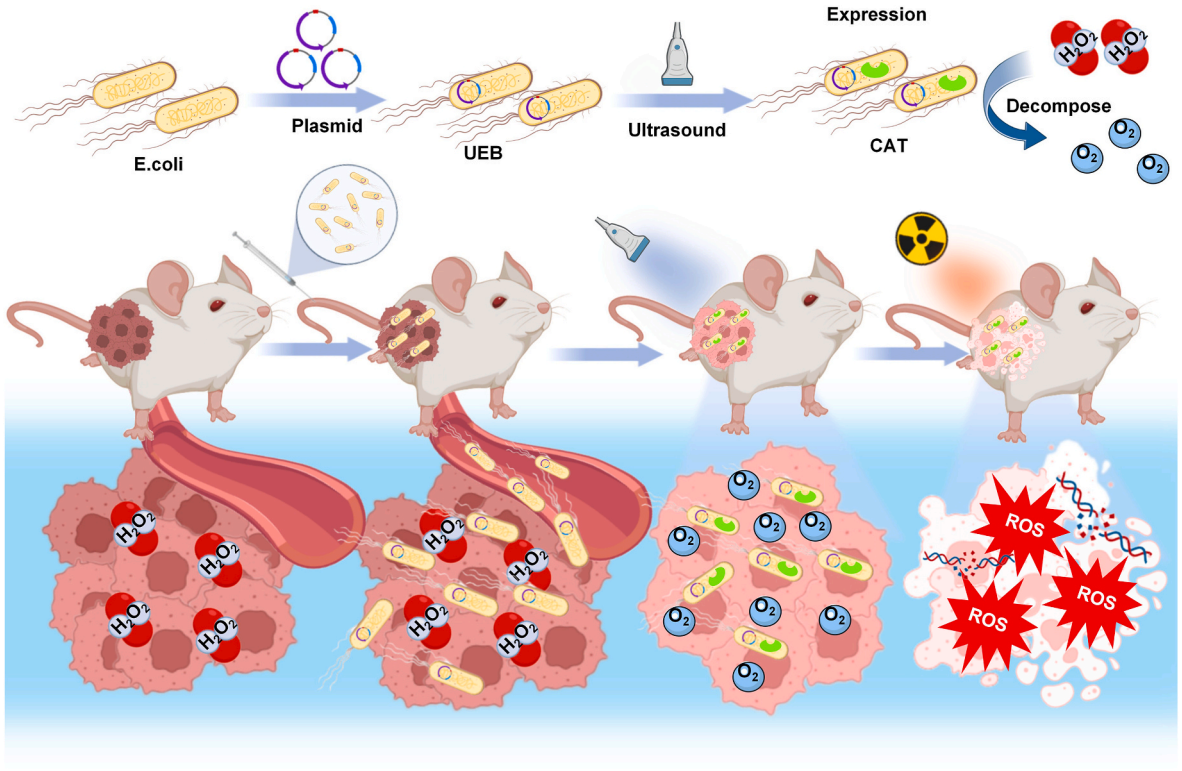

Fig. 1. Schematic diagram of ultrasound-responsive engineered bacteria (UEB) designed to enhance the efficiency of radiotherapy. These engineered bacteria target tumors and express catalase (CAT) to increase oxygen and alleviate hypoxia. UEB, activated by ultrasound, enhances O_2 levels in tumors, promoting DNA damage, and ROS generation, and improving radiotherapy effectiveness by reducing tumor volume and inducing apoptosis and necrosis.

by Tsingke Biotechnology Co., Ltd. (Beijing, China). This plasmid contains a gene fragment encoding a codon-optimized sequence for Escherichia coli. Isopropyl-β-D-1-thiogalactopyranoside (IPTG) induces the expression of CAT by regulating the constitutive T7 promoter. The preparation of IEB followed a procedure similar to that used for UEB [25].

2.3. Animal model

Female BALB/c mice, aged 6–8 weeks, were obtained from Beijing Vital River Laboratory Animal Technology Co., Ltd. (China). These animals were housed under optimal temperature and humidity conditions. To induce the formation of 4T1 tumor models, each mouse received a subcutaneous injection of 1×10^6 4T1 cells suspended in 100 μL of serum-free medium in the right flank.

2.4. US-responsive CAT expression and hypoxia relief of UEB

The UEB was cultured at 30 °C to OD600 0.4–0.6, then expose it to US (1 MHz, 0.4 W/cm^2, 80 % duty cycle) for 2 h, to ensure that the thermal effects generated by US under these parameters could elevate the temperature to 42 °C. CAT expression was analyzed via SDS-PAGE. CAT activity was measured with the Catalase (CAT) assay kit (Nanjing Jiancheng Bioengineering Institute). Oxygen solubility was measured using a portable dissolved oxygen meter (Shanghai INESA Scientific Instruments Co., Ltd). UEB accumulation in organs was assessed by colony counting. Tumor-bearing mice were divided into groups: control, E. coli, E. coli + US, UEB, and UEB + US. Ultrasound (1 MHz, 0.4 W/cm^2, 80 % duty cycle) was applied 48 h post-injection. Tumor tissues were analyzed for CAT activity and HIF-1α via immunofluorescence using the EVOS M7000 system.

2.5. Spatiotemporal CAT expression of UEB by US

In vitro, UEB, IEB, and IEB + IPTG were prepared, with bacterial liquid soaked in black cardboard. Groups included IEB, IEB + IPTG, UEB, and UEB + US. After 30 min of ultrasound (1 MHz, 0.4 W/cm^2, 80 % duty cycle), cardboard was immersed in 3 % H_2O_2, and oxygen production was measured by photographing after 1 min. In vivo, mice with 400 mm^3 tumors were divided into UEB + US and IEB + IPTG groups. Mice in UEB + US received 1×10^7 bacteria and ultrasound 48 h post-injection. Mice in IEB + IPTG received 1×10^7 IEB with IPTG. After 24 h, organs and tumor tissues were collected for SDS-PAGE and Western blotting (His-tag, 1:3000, ImmunoWay). Protein density was quantified using ImageJ.

2.6. Intracellular reactive ROS generation

4T1 cells (5×10^4 cells/well) were cultured under normoxic and hypoxic conditions for 24 h. Four experimental groups (n = 3) were established: Control, RT, UEB + RT, and UEB + US + RT. Two hours before RT, 2 μl of 3 % H_2O_2 was added to each group. In the UEB + RT group, 1×10^6 CFU of UEB was added, while in the UEB + US + RT group, UEB irradiated with US (1 MHz, 0.4 W/cm^2, 80 % duty cycle) for 30 min was administered, thereby avoiding the impact of ultrasound-induced mechanical effects on the growth of 4T1 cells. After 2 h, RT groups were exposed to 10 Gy. ROS levels were assessed using the EVOS M7000 microscope and flow cytometry, analyzed by FlowJo 10.8.

2.7. γ-H2AX immunofluorescence analysis

Cells were processed as in the ROS generation method. After treatment, γ-H2AX expression was detected using a commercial kit, and foci density (foci/100 μm^2) was quantified using ImageJ software.

2.8. CCK-8 assay

4T1 cells (1×10^4 cells/well) were plated in 96-well plates. In the UEB + RT and UEB + US + RT groups, 5×10^5 CFU of UEB were added. Six hours after 10Gy radiation, cell viability was assessed using the CCK-8 assay, and absorbance was measured spectrophotometrically.

2.9. In vivo tumor treatment

Tumor-bearing mice (400 mm^3) were divided into five groups (n = 4): PBS, PBS + RT, UEB + US + RT, UEB + RT, and UEB + US. Mice in the UEB groups received intravenous 1×10^7 CFU of UEB, and UEB + US + RT and UEB + US groups underwent 30 min of ultrasound irradiation. Simultaneously, it was ensured that mice in the UEB + US + RT group received US irradiation again before each RT session. Mice were treated with 2 Gy RT on days 0, 3, 6, and 9, and tumor volumes were measured. After euthanasia, organs and tumors were harvested for analysis. TUNEL and H&E staining were performed, and serum ALT, CREA, and BUN levels were measured.

2.10. Statistical analysis

The statistical analyses of experiment data were conducted utilizing GraphPad Prism software version 9.5.0. The data set was subjected to a one-way analysis of variance (ANOVA) for statistical evaluation, and the P values were determined by employing a two-tailed unpaired heteroscedastic *t*-test, with significance indicated by *P < 0.05, **P < 0.01, and ***P < 0.001, ****P < 0.0001.

3. Results

3.1. US-responsive UEB to express CAT and alleviate the hypoxic TME

The design goals of UEB are to express CAT and effectively decompose H_2O_2 into O_2, thus alleviating tumor hypoxia (Fig. 2A). The agarose gel electrophoresis results of the recombinant plasmid revealed a fragment of approximately 2000 bp, which matches the expected size of the CAT fragment (1608 bp), confirming the successful insertion of the CAT gene into the bacterial plasmid (Fig. S1). SDS-PAGE result indicated that UEB efficiently produced CAT protein after ultrasound irradiation, while UEB cultured at 30 °C under normal conditions did not (Fig. 2B). Furthermore, considering the bioactivity of UEB after radiation irradiation, the result of monoclonal colony counting revealed that no significant changes in colony numbers after 10 Gy irradiation (Fig. 2C), and SDS-PAGE gel electrophoresis confirmed that UEB could still produce CAT after 10 Gy radiation (Fig. S2). These findings support the ability of UEB to continuously express CAT with RT in vivo. Then, the ability of UEB to catalyze H_2O_2 degradation and yield O_2 was assessed. The CAT activity in the UEB + US group (46.07 U/ml) was significantly higher than E. coli (12.49 U/ml), UEB (17.16 U/ml), and the E. coli + US group (15.65 U/ml), the CAT activity in the UEB + US group was approximately 2.7 times that of the UEB group, indicating that US can significantly enhance the expression of CAT in UEB (Fig. 2D). The oxygen concentration in the UEB + US group increased to 78.26 mg/L at 2 min, maintaining this level for 6 min, while other groups peaked at lower levels. There is no significant difference in O_2 levels detected in E. coli, UEB, and the E. coli + US groups, whereas significantly higher levels of O_2 were detected in UEB + US group (Fig. 2E).

For active tumor-targeted delivery, UEB was intravenously injected into 4T1 tumor-bearing mice. Bacterial plate inoculation was performed on homogenates of their tissues and organs, revealing a significantly higher number of bacterial colonies in tumor tissues compared to other organs. This indicates that UEB can target and accumulate within tumor tissues, demonstrating its distribution profile in vivo (Fig. S3). CAT activity in the tumor tissue was significantly elevated in the UEB + US group (Fig. 2F), and HIF-1α expression analysis showed that UEB + US

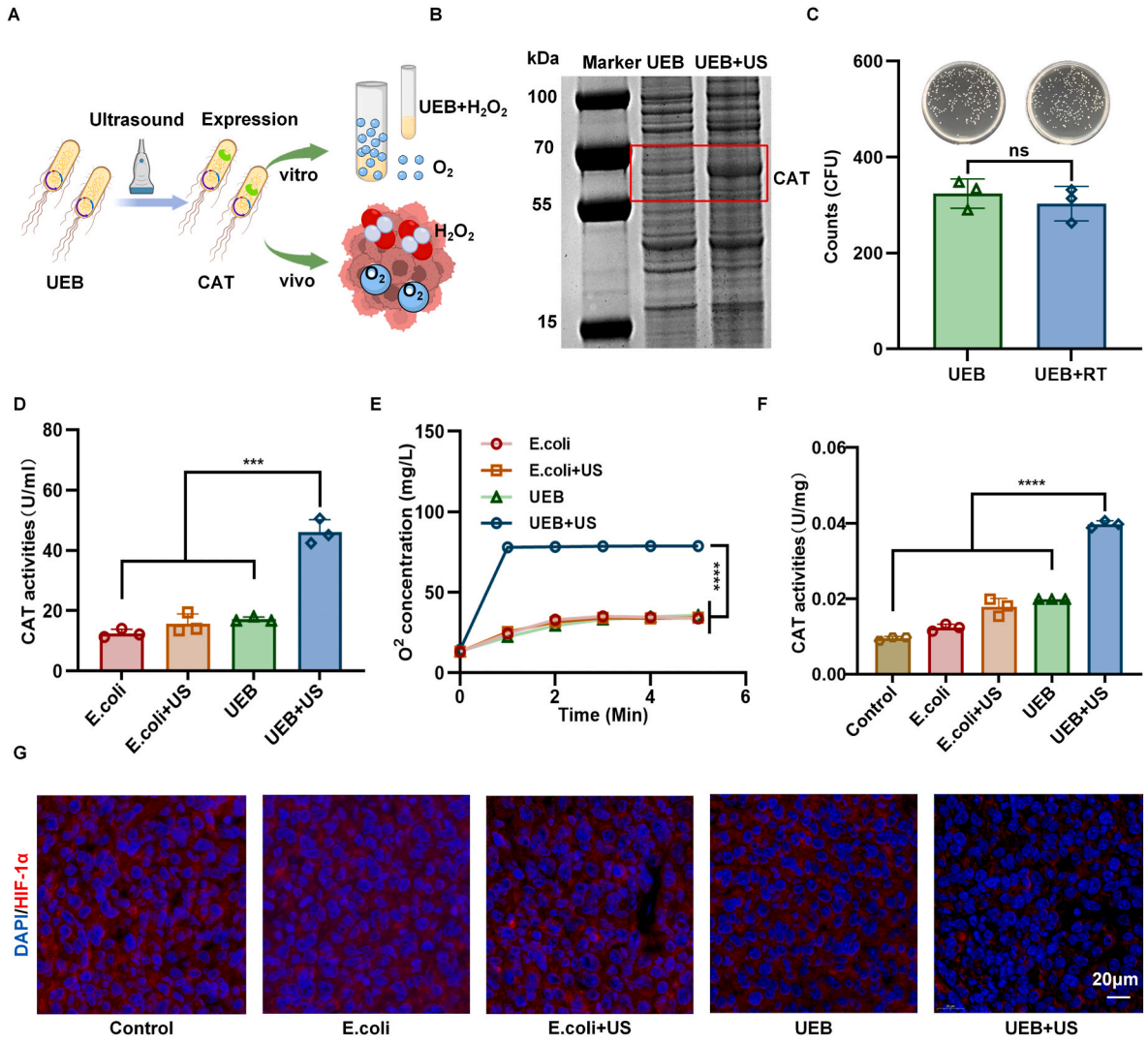

Fig. 2. Functional validation of ultrasound-responsive gene expression in UEB. A, UEB was engineered to express CAT, decompose H_2O_2 into O_2 via ultrasound, and target tumors to alleviate hypoxia. **B,** SDS-PAGE images demonstrating CAT expression in UEB. **C,** Colony count of UEB before and after 10Gy irradiation. **D,** In vitro CAT activity of bacterial strains activated by ultrasound (n = 3). **E,** H_2O_2 decomposition by bacterial strains under ultrasound (n = 3). **F,** In vivo CAT activity in tumor tissue (n = 3). **G,** Immunofluorescence of HIF-1α in tumor tissue (n = 3, scale bar = 20 μm). Statistical analysis was performed using one-way ANOVA and Tukey's test (****P < 0.0001; ***P < 0.001).

treatment alleviated tumor hypoxia compared to other groups (Fig. 2G), demonstrated that US can efficiently regulate the expression of CAT in UEB in vivo, exhibiting excellent activity and functionality. The analysis of HIF-1α fluorescence intensity using ImageJ also corroborated these findings (Fig. S4).

3.2. *Verification of spatiotemporal control of CAT expression by US*

To compare the effects of different induction techniques on bacterial activity, we measured the OD of IEB and UEB. The results indicate that the UEB + US group exhibited a higher OD compared to the UEB group, while the IEB + IPTG group demonstrated a lower OD than the IEB group. This suggests that ultrasound irradiation promotes bacterial growth, whereas IPTG has a slight inhibitory effect on growth (Fig. 3A). Subsequently, we mapped the regions of CAT expression in engineered bacteria, which decompose H_2O_2 and produce oxygen (Fig. 3B). Gas bubble production was observed exclusively within the ultrasound-irradiated circular area of the UEB + US group, while the IEB + IPTG group exhibited bubble production across the entire black background. Conversely, both the UEB and IEB groups showed minimal gas bubble production (Fig. 3C). This indicates that UEB only decomposes H_2O_2 through the action of CAT within the region of US irradiation when US is applied. US enables the spatiotemporally controlled expression of CAT in UEB, whereas IEB + IPTG lacks the capability to spatially control the expression of CAT.

Western blot analysis further confirmed whether US can specifically and efficiently activate bacterial protein expression in vivo. Significant CAT expression was detected solely in the tumor tissue of the UEB + US group, whereas the IEB + IPTG group exhibited CAT expression across all tissues and organs. Notably, the UEB + US group showed lower levels of CAT protein in normal tissues but higher levels in tumor tissues compared to the IEB + IPTG group. In the IEB + IPTG group, the liver displayed the second-highest CAT protein levels, followed by the lungs, while the heart exhibited the lowest levels. This trend aligns with the findings in the UEB + US group. Further quantitative analysis of gray levels using ImageJ software confirmed the specificity of ultrasound regulation in vivo (Fig. 3D and E).

3.3. *UEB-mediated radiosensitization controlled by ultrasound in vitro*

Using a radiation dose of 10Gy, the immunofluorescence analysis revealed that under normoxic conditions, there was no significant

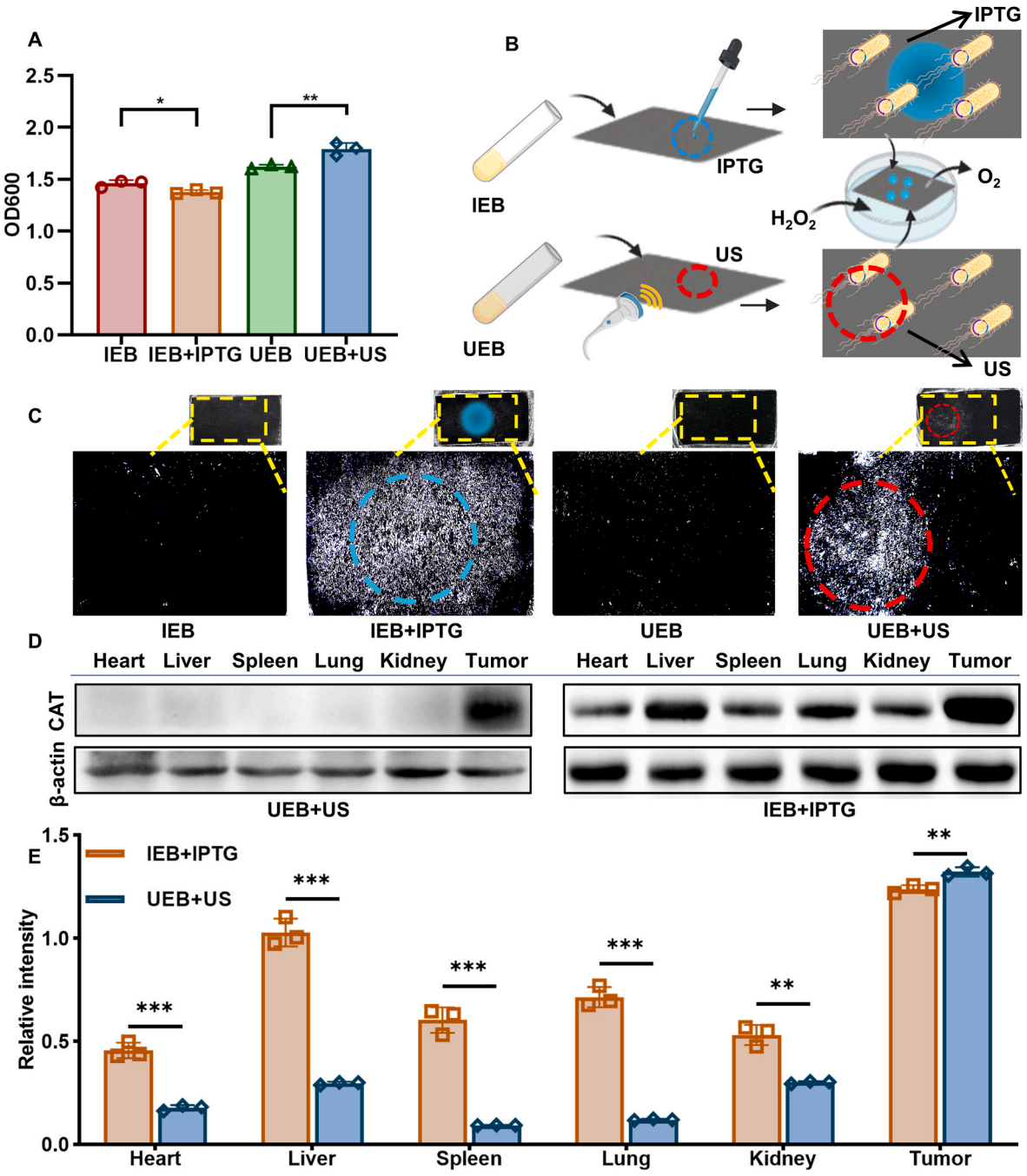

Fig. 3. Comparison of Different Methods for Inducing Bacterial Protein Expression. A, Effects of different induction methods on bacterial survival (n = 3). **B,** Experimental design for the in vitro protein induction validation. **C,** Validation of specific CAT expression in UEB and IEB in vitro. **D-E,** WB analysis**(D)** and densitometric quantification **(E)** of CAT expression in vivo using β-actin as control. Protein quantification was performed using densitometry via ImageJ software (n = 3). Statistical analysis was performed using one-way ANOVA and Tukey's test (****P < 0.0001, ***P < 0.001, **P < 0.01; *P < 0.05).

difference in the fluorescence intensity of γ-H2AX among the RT group, UEB + RT group, and UEB + US + RT group after RT, indicating that tumors are highly sensitive to RT when oxygen is sufficient. Under hypoxic conditions, the fluorescence intensity of γ-H2AX in the UEB + US + RT group significantly increased after RT, suggesting that RT alone cannot cause significant DNA damage in cells under hypoxia. However, after treatment with UEB + US, the DNA damage in cells was enhanced (Fig. 4A). Quantitative analysis of fluorescence intensity using ImageJ software corroborated these findings (Figs. S5–6). Next, the ability of UEB to influence the production of ROS in cells under RT was evaluated. Under normoxia, intense green fluorescence was observed in the RT, UEB + RT, and UEB + US + RT groups, indicating ROS production, with tumor cells displaying significant fluorescence. In contrast, under hypoxic conditions, only the UEB + US + RT group showed noticeable fluorescence. The RT and UEB + RT groups exhibited minimal fluorescence (Fig. 4B). Flow cytometry revealed that under hypoxic conditions, the fluorescence intensity of the UEB + US + RT group reached approximately 14,000, whereas both the RT and UEB + RT groups had intensities around 3000 (Fig. 4C–E). CCK-8 assays showed that under hypoxia, a cellular RT effect could be triggered for cells treated with UEB in normoxia condition. In contrast, RT efficacy was limited by hypoxia, with cell viability around 80 % in the RT and UEB + RT groups. The UEB + US + RT group had reduced viability (62 %), similar to normoxic conditions, indicating a radiosensitizing effect (Fig. 4F). Under long-

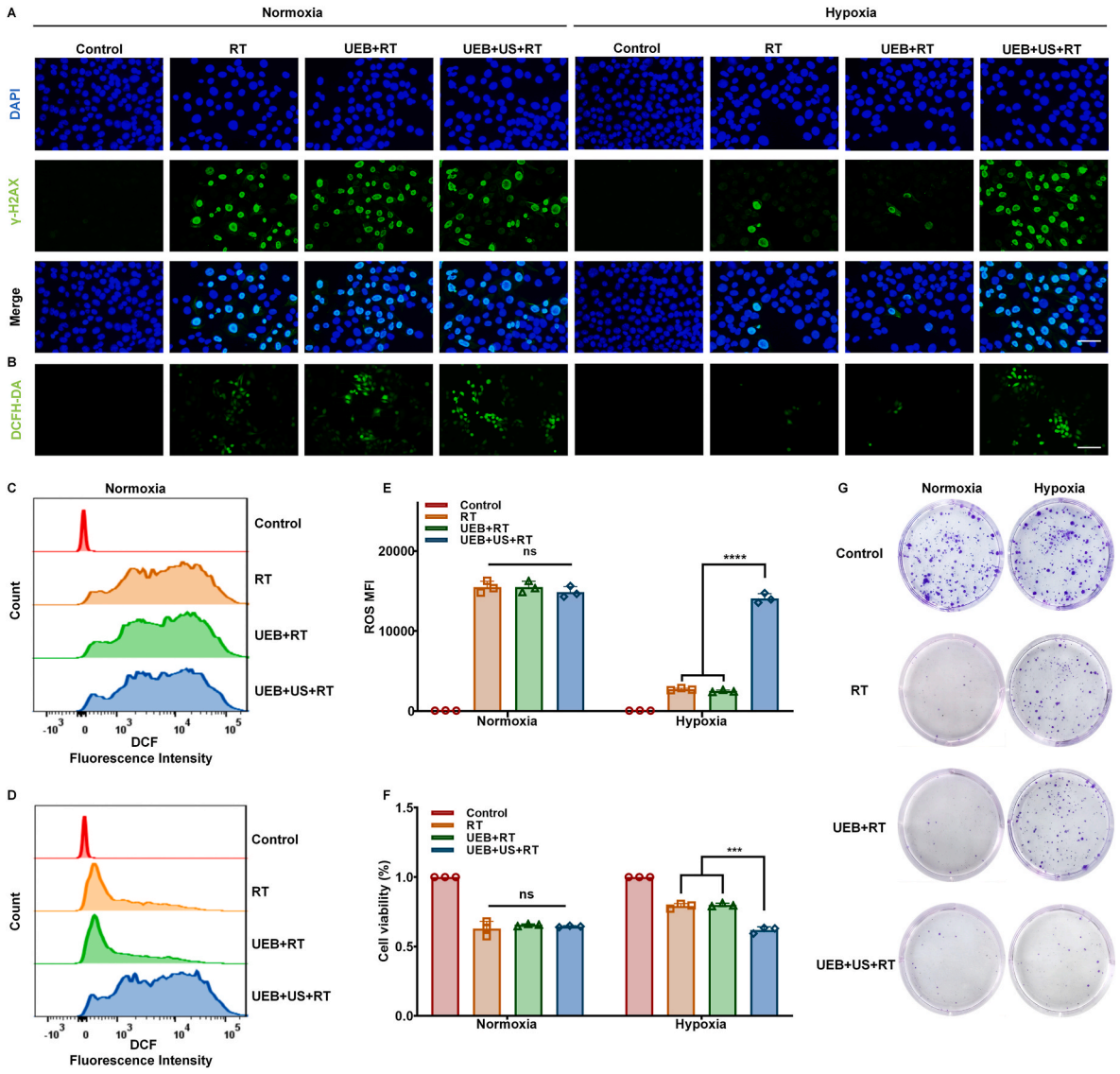

Fig. 4. In Vitro Radiosensitizing Effect of UEB. A, DAPI, and γ-H2AX staining show nuclear condensation and DNA breaks under normoxia and hypoxia (scale bar = 150 μm). **B,** ROS generation using DCFH-DA under normoxia and hypoxia (scale bar = 275 μm). **C-E,** Flow cytometric profiles under normoxia**(C)** or hypoxia**(D),** and DCF fluorescence intensity was analyzed to quantify ROS generation by using FlowJo **(E)** (n = 3). **F,** CCK-8 assays for cell viability changes under normoxia and hypoxia (n = 3). **G,** Colony formation of 4T1 cells treated with 10 Gy radiation. Statistical analysis was performed using one-way ANOVA and Tukey's test (****P < 0.0001; ***P < 0.001).

term culture conditions, DNA breaks could self-repair, leading to the survival of most cells. Colony formation assays under hypoxia showed fewer colonies in the UEB + US + RT group, similar to those receiving radiation treatment under normoxia, while control group cells proliferated normally. These findings demonstrate the pronounced radiosensitizing ability of UEB + US + RT under hypoxic conditions (Fig. 4G).

3.4. *UEB-mediated radiosensitization controlled by ultrasound in vivo*

To evaluate the in vivo radiosensitizing effects of UEB combined with RT, tumor-bearing mice were treated with different methods (Fig. 5A). In the UEB + US + RT group, tumor volume was significantly reduced, averaging 96.2 mm^3 on day 22, compared to 312.8 mm^3 (PBS + RT) and 320.5 mm^3 (UEB + RT). Tumor volumes in the PBS and UEB + US groups increased to about 1100 mm^3 (Fig. 5B and C). Tumor weights were lowest in the UEB + US + RT group (0.2 g) and highest in the PBS group (1.47 g). This indicates a sevenfold increase in tumor weight compared to the UEB + US + RT treatment (Fig. 5D). Histological examinations of necrosis and apoptosis in tumor tissues were conducted using H&E staining and TUNEL assays. H&E staining revealed more pronounced nuclear dissolution and karyorrhexis in the tumor tissues of mice treated with UEB + US + RT, accompanied by significantly enlarged intercellular spaces. Concurrently, TUNEL assays demonstrated a markedly higher level of red fluorescence in the tumor tissues of mice treated with UEB + US + RT compared to those subjected to other treatments, indicating a significant increase in apoptotic cells (Fig. 5E and F).

Safety assessments showed normal liver and kidney function (ALT, CREA, BUN) in both PBS and UEB + US + RT groups (Figs. S7–9), and no evident inflammation or histological changes were observed in the organs of mice treated with UEB + US + RT (Fig. S10). These results demonstrate the safety of the therapeutic strategy utilizing ultrasound-regulated CAT expression in UEB to achieve tumor radiosensitization.

4. Discussion

Tumor hypoxia has long been thought of a critical challenge in cancer therapy, and addressing this issue is of paramount importance for

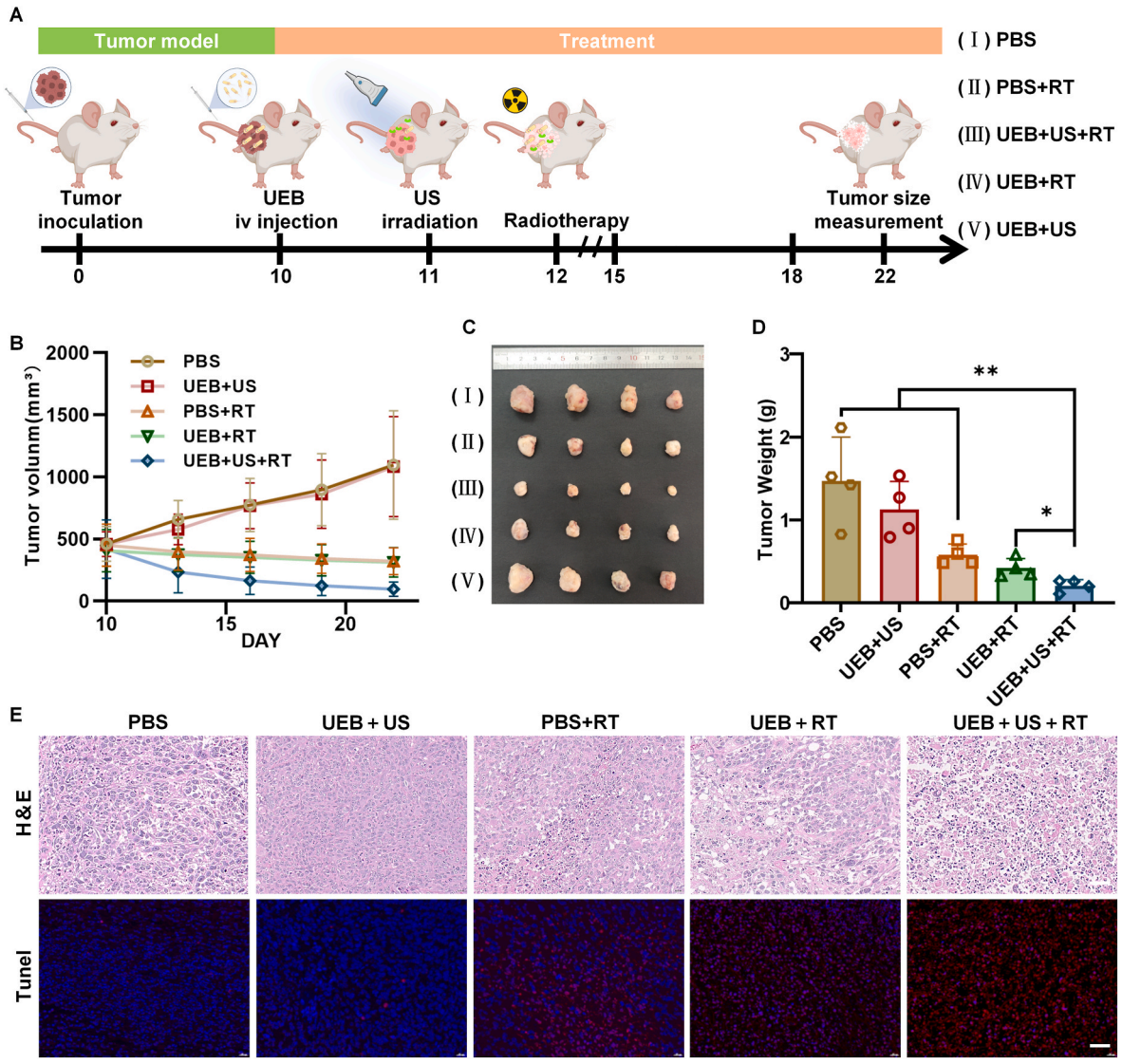

Fig. 5. Tumor radiosensitization in vivo mediated by UEB. A, Schematic diagram illustrating the treatment model for tumor radiosensitization mediated by UEB in the 4T1 tumor-bearing mouse model. **B,** Tumor growth curves under various treatment conditions (n = 4). **C,** Images of tumors across different treatment conditions (n = 4). **D,** Tumor weights in the various treatment groups (n = 4). **E-F,** H&E **(E)**, and TUNEL **(F)** staining of tumors from each group (scale bar = 20 μm). Statistical analysis was conducted using one-way ANOVA and Tukey's test (****P < 0.0001; **P < 0.01; *P < 0.05).

improving therapy efficiency [26]. The excessive H_2O_2 present in tumor tissues is a type of ROS with relatively weak oxidative capacity, which to some extent promotes tumor progression [27]. When H_2O_2 decomposes to produce O_2, under radiation, the O_2 generates a large amount of highly oxidative ROS (such as •OH), leading to severe DNA damage and inducing cell death [28]. In this study, UEB was developed for spatio-temporally controlling CAT expression. We cloned the target CAT gene fragment into the pBV220 plasmid vector harboring a temperature-sensitive promoter and transfected it into MG1655 for gene amplification and protein expression. MG1655 possesses a fully sequenced genome, a well-defined genetic background, and higher transformation efficiency, which facilitate stable plasmid integration and expression regulation. Additionally, its lower metabolic burden makes it more suitable for the efficient expression of exogenous genes on the pBV220 plasmid. Utilizing established genetic tools and the research foundation laid by our team, the successful insertion and expression of pBV220-CAT were ensured [29–31]. By adjusting US parameters and irradiation range, we precisely controlled the tumor temperature to rise to 42 °C, thereby initiating the transcriptional expression of the CAT gene, which decomposes H_2O_2 to produce O_2. This method alleviates hypoxia in TME and enhances the therapeutic efficacy of RT for breast cancer. In the process of detecting the expression of CAT in UEB, we observed an increase in CAT activity in the E. coli + US group. This result may be due to the cavitation effect of US irradiation, which increases the permeability of the cell membrane, allowing substances such as hydrogen peroxide to enter E. coli, thereby inducing the expression and upregulation of CAT enzyme activity to activate the antioxidant defense system [32,33]. Furthermore, we observed that US irradiation promoted the growth of UEB. This phenomenon may be attributed to the thermal effects and mechanical vibrations generated by US irradiation. The thermal effects of US increased the temperature of the bacterial suspension, accelerating enzymatic activity and metabolic reactions, thereby promoting cell division. Additionally, mechanical vibrations enhanced the permeability of the cell membrane and improved the efficiency of material exchange in the local microenvironment [34,35]. In our experiments, we observed that although both in vivo and in vitro studies demonstrated the radiosensitizing effect of UEB + US, the efficacy of RT under hypoxic conditions was weaker in vitro compared to in vivo, where a certain therapeutic effect was still evident. This discrepancy may be attributed to the strictly controlled hypoxic conditions in

the in vitro experiments, whereas the presence of non-hypoxic regions in in vivo tumors enhances their sensitivity to RT. It is challenging to replicate the complex vascularized regions, immune cell infiltration, and interactions among various cytokines and metabolites present in solid tumors in vitro [36]. Additionally, we considered that the Annexin V-FITC/PI probe might be affected by UEB, and therefore did not use flow cytometry to validate the sensitizing effect of UEB + US on radiation-induced apoptosis [37]. All in all, this strategy presented a novel approach for enhancement of cancer cell apoptosis induced by RT and significantly inhibiting tumor growth, thus exciting new insights for cancer therapy.

Targeting the hypoxic TME through CAT delivery was allowed for the decomposition of excessive H_2O_2, thus alleviating hypoxia [38]. In our initial studies, we observed that MG1655 demonstrates significant active targeting efficacy and substantial tissue retention within tumor tissues. Following the injection of MG1655 into mice, the bacterial colony count in tumor tissues exhibited exponential growth over time, peaking at 7 days and subsequently declining. Bacterial colonies were still observed in tumor tissues at 14 and 21 days, whereas colonies in other tissues gradually diminished over time [24]. In this study, the tumor-targeting ability of UEB was also evaluated, with UEB exhibiting notable and active tumor-targeting efficacy and selective accumulation. This phenomenon is primarily attributed to the characteristics of TME and the biological features of UEB. The highly permeable vasculature of tumor tissues creates conditions for UEB to infiltrate the tumor. The low pH, complex composition, and immunosuppressive nature of TME enhance the invasiveness and tropism of UEB toward tumor tissues, while also aiding UEB in evading immune clearance. Additionally, UEB, as a facultative anaerobe, is capable of surviving and proliferating in the hypoxic TME [39]. Next, we demonstrated that UEB subjected to US irradiation significantly enhanced CAT activity at the tumor site, ameliorated the hypoxic tumor microenvironment, and suppressed the expression of HIF-1α. By performing US irradiation prior to RT, we induced UEB to express CAT, thereby alleviating the hypoxic TME and increasing the sensitivity of tumors to RT. With a substantial increase in the catalytic activity for H_2O_2 decomposition, UEB showed a potential of producing large amounts of CAT to realize a substantial generation of oxygen in vitro. This not only aligns with previous studies by Huang et al. in engineering bacteria to alleviate tumor hypoxia, but also further underscores the potential of genetic engineering in bacterial-based therapeutic applications [40]. It is a highly efficient method for addressing tumor hypoxia and provides a promising strategy for overcoming this critical issue in cancer treatment was represented by UEB.

Despite the advances made, achieving specific temporal and spatial control of protein expression in bacteria remains a challenge [41,42]. In this research, it was successfully demonstrated the unique advantages of ultrasound as a physical stimulus for activating gene expression, achieving precise spatiotemporal control of CAT expression. Compared to other type of induction methods, such as IPTG based chemical induction, ultrasound possessed the advantage of high specificity and spatiotemporal controllability [43,44]. It also overcomes the potential damage caused by radiation exposure and the limitations of light-based stimulation in reaching deep tumors [45,46]. Furthermore, unlike biological methods, which are influenced by population density and face challenges in achieving precise spatial and temporal control in vivo, ultrasound was thought to offer excellent precision in this regard, providing a promising tool for personalized medicine [47]. For example, similar to the study by Yang et al., which employed engineered bacteria with specific plasmids to control gene expression via ultrasound in tumor-targeting bacteria, the effectiveness of this method in improving therapeutic outcomes was further validated by this work [48]. Despite the promising results, the application of UEB still faces safety concerns for clinical applications. The application of non-pathogenic or attenuated bacterial strains and a quorum sensing-mediated autolytic system should be considered for self-elimination in future clinical applications. The hypoxia-relief strategy should also be refined with the combination of other therapies like photodynamic therapy. Additionally, engineered bacteria can enhance immune cell infiltration in tumor tissues through surface components such as lipopolysaccharides, thereby activating the anti-tumor immune system. Future studies should further explore the impact of engineered bacteria on the host immune system to potentially combine with immunotherapy and achieve greater therapeutic efficacy against tumors [49]. In summary, the strategy of using UEB combined with focused ultrasound to alleviate deep tumor hypoxia has shown considerable potential. However, more in-depth research is needed to address safety concerns, optimize combination therapies, to advance its clinical application.

CRediT authorship contribution statement

Zichao Liu: Writing – review & editing, Visualization, Validation, Methodology, Investigation, Formal analysis, Data curation, Conceptualization. **Lingling Lei:** Writing – review & editing, Writing – original draft, Visualization, Validation, Investigation, Formal analysis, Data curation. **Zenan Zhang:** Validation, Data curation. **Meng Du:** Writing – review & editing, Supervision, Resources, Funding acquisition, Conceptualization. **Zhiyi Chen:** Writing – review & editing, Supervision, Resources, Project administration, Funding acquisition.

Ethics approval statement

All animal experiments complied with ARRIVE guidelines and received approval from the Medical Ethics Committee at the University of South China (The approval number: USC2024XS267). Animal-related procedures adhered to ethical guidelines established by the Experimental Animal Welfare Ethics Committee of the University of South China.

Funding

This work was supported by the National Natural Science Foundation of China (grant numbers 82272028, 82102087), and the Hunan Provincial Health High-Level Talent Scientific Research Project (grant number R2023010).

Declaration of competing interest

The authors declare that they have no known competing financial interests or personal relationships that could have appeared to influence the work reported in this paper.

Appendix A. Supplementary data

Supplementary data to this article can be found online at https://doi.org/10.1016/j.mtbio.2025.101620.

Data availability

Data will be made available on request.

References

[1] H. Sung, J. Ferlay, R.L. Siegel, M. Laversanne, I. Soerjomataram, A. Jemal, F. Bray, Global cancer statistics 2020: GLOBOCAN estimates of incidence and mortality worldwide for 36 cancers in 185 countries, CA Cancer J. Clin. 71 (3) (2021) 209–249, https://doi.org/10.3322/caac.21660.

[2] Y. Zu, Z. Wang, H. Yao, L. Yan, Oxygen-generating biocatalytic nanomaterials for tumor hypoxia relief in cancer radiotherapy, J. Mater. Chem. B 11 (14) (2023) 3071–3088, https://doi.org/10.1039/d2tb02751h.

[3] S. Kim, A. Sundaram, A.P. Mathew, V.S. Hareshkumar, A. Mohapatra, R. G. Thomas, T.T.M. Bui, K. Moon, S. Kweon, I.-K. Park, Y.Y. Jeong, In situ hypoxia modulating nano-catalase for amplifying DNA damage in radiation resistive colon tumors, Biomater. Sci. 11 (18) (2023) 6177–6192, https://doi.org/10.1039/d3bm00618b.

[4] Z. Guo, P.E. Saw, S. Jon, Non-invasive physical stimulation to modulate the tumor microenvironment: unveiling a new frontier in cancer therapy, BIO Integration 5 (1) (2024), https://doi.org/10.15212/bioi-2024-0012.
[5] T. Suwa, M. Kobayashi, J.-M. Nam, H. Harada, Tumor microenvironment and radioresistance, Exp. Mol. Med. 53 (6) (2021) 1029–1035, https://doi.org/10.1038/s12276-021-00640-9.
[6] Y. Pan, L. Liu, X. Mou, Y. Cai, Nanomedicine strategies in conquering and utilizing the cancer hypoxia environment, ACS Nano 17 (21) (2023) 20875–20924, https://doi.org/10.1021/acsnano.3c07763.
[7] C. Ruan, K. Su, D. Zhao, A. Lu, C. Zhong, Nanomaterials for tumor hypoxia relief to improve the efficacy of ROS-generated cancer therapy, Front. Chem. 9 (2021), https://doi.org/10.3389/fchem.2021.649158.
[8] D.W. Zheng, B. Li, C.X. Li, J.X. Fan, Q. Lei, C. Li, Z. Xu, X.Z. Zhang, Carbon-dot-decorated carbon nitride nanoparticles for enhanced photodynamic therapy against hypoxic tumor via water splitting, ACS Nano 10 (9) (Sep 27 2016) 8715–8722, https://doi.org/10.1021/acsnano.6b04156.
[9] R.P. Accolla, J.P. Liang, T.R. Lansberry, I.L. Miravet, M. Loaisiga, B.L. Sardi, C. L. Stabler, Engineering modular, oxygen-generating microbeads for the in situ mitigation of cellular hypoxia, Adv. Healthcare Mater. 12 (19) (Jul 2023) e2300239, https://doi.org/10.1002/adhm.202300239.
[10] J.J. Bosque, G.F. Calvo, V.M. Pérez-García, M.C. Navarro, The interplay of blood flow and temperature in regional hyperthermia: a mathematical approach, R. Soc. Open Sci. 8 (1) (Jan 2021) 201234, https://doi.org/10.1098/rsos.201234.
[11] N. Yang, W. Xiao, X. Song, W. Wang, X. Dong, Recent advances in tumor microenvironment hydrogen peroxide-responsive materials for cancer photodynamic therapy, Nano-Micro Lett. 12 (1) (2020), https://doi.org/10.1007/s40820-019-0347-0.
[12] Q. Liu, A. Zhang, R. Wang, Q. Zhang, D. Cui, A review on metal- and metal oxide-based nanozymes: properties, mechanisms, and applications, Nano-Micro Lett. 13 (1) (2021), https://doi.org/10.1007/s40820-021-00674-8.
[13] L. Yu, Z. Liu, W. Xu, K. Jin, J. Liu, X. Zhu, Y. Zhang, Y. Wu, Towards overcoming obstacles of type II photodynamic therapy: endogenous production of light, photosensitizer, and oxygen, Acta Pharm. Sin. B 14 (3) (2024) 1111–1131, https://doi.org/10.1016/j.apsb.2023.11.007.
[14] J. Zhu, A. Jiao, Q. Li, X. Lv, X. Wang, X. Song, B. Li, Y. Zhang, X. Dong, Mitochondrial Ca2+-overloading by oxygen/glutathione depletion-boosted photodynamic therapy based on a CaCO3 nanoplatform for tumor synergistic therapy, Acta Biomater. 137 (2022) 252–261, https://doi.org/10.1016/j.actbio.2021.10.016.
[15] X. Huang, J. Pan, F. Xu, B. Shao, Y. Wang, X. Guo, S. Zhou, Bacteria-based cancer immunotherapy, Adv. Sci. 8 (7) (2021), https://doi.org/10.1002/advs.202003572.
[16] C. R, Arpaia N. Gurbatri, T. Danino, Engineering bacteria as interactive cancer therapies, Science 378 (6622) (2022) 858–864, https://doi.org/10.1126/science.add9667.
[17] M. Du, T. Wang, W. Peng, R. Feng, M. Goh, Z. Chen, Bacteria-driven nanosonosensitizer delivery system for enhanced breast cancer treatment through sonodynamic therapy-induced immunogenic cell death, J. Nanobiotechnol. 22 (1) (2024), https://doi.org/10.1186/s12951-024-02437-0.
[18] S. Ding, Z. Liu, C. Huang, N. Zeng, W. Jiang, Q. Li, Novel engineered bacterium/black phosphorus quantum dot hybrid system for hypoxic tumor targeting and efficient photodynamic therapy, ACS Appl. Mater. Interfaces 13 (8) (2021) 10564–10573, https://doi.org/10.1021/acsami.0c20254.
[19] M. Zamocky, P.G. Furtmüller, C. Obinger, Evolution of catalases from bacteria to humans, Antioxidants Redox Signal. 10 (9) (Sep 2008) 1527–1548, https://doi.org/10.1089/ars.2008.2046.
[20] G. Wu, Q. Yan, J.A. Jones, Y.J. Tang, S.S. Fong, M.A.G. Koffas, Metabolic burden: cornerstones in synthetic biology and metabolic engineering applications, Trends Biotechnol. 34 (8) (2016) 652–664, https://doi.org/10.1016/j.tibtech.2016.02.010.
[21] M.-R. Wu, B. Jusiak, T.K. Lu, Engineering advanced cancer therapies with synthetic biology, Nat. Rev. Cancer 19 (4) (2019) 187–195, https://doi.org/10.1038/s41568-019-0121-0.
[22] N.S. Forbes, Engineering the perfect (bacterial) cancer therapy, Nat. Rev. Cancer 10 (11) (2010) 785–794, https://doi.org/10.1038/nrc2934.
[23] L. Lin, Y. Fan, F. Gao, et al., UTMD-promoted Co-delivery of gemcitabine and miR-21 inhibitor by dendrimer-entrapped gold nanoparticles for pancreatic cancer therapy, Theranostics 8 (7) (2018) 1923–1939, https://doi.org/10.7150/thno.22834.
[24] Y. Chen, M. Du, Z. Yuan, Z. Chen, F. Yan, Spatiotemporal control of engineered bacteria to express interferon-γ by focused ultrasound for tumor immunotherapy, Nat. Commun. 13 (1) (Aug 2 2022) 4468, https://doi.org/10.1038/s41467-022-31932-x.
[25] T. Wang, M. Du, Z. Yuan, J. Guo, Z. Chen, Multi-functional nanosonosensitizer-engineered bacteria to overcome tumor hypoxia for enhanced sonodynamic therapy, Acta Biomater. 189 (2024) 519–531, https://doi.org/10.1016/j.actbio.2024.10.013.
[26] D. Han, X. Zhang, Y. Ma, X. Yang, Z. Li, The development of live microorganism-based oxygen shuttles for enhanced hypoxic tumor therapy, Mater Today Bio 18 (2023), https://doi.org/10.1016/j.mtbio.2022.100517.
[27] F.J. Lei, J.Y. Chiang, H.J. Chang, D.C. Chen, H.L. Wang, H.A. Yang, K.Y. Wei, Y. C. Huang, C.C. Wang, S.T. Wei, C.H. Hsieh, Cellular and exosomal GPx1 are essential for controlling hydrogen peroxide balance and alleviating oxidative stress in hypoxic glioblastoma, Redox Biol. 65 (2023) 102831.65, https://doi.org/10.1016/j.redox.2023.102831.
[28] Y. Chen, H. Zhong, J. Wang, X. Wan, Y. Li, W. Pan, N. Li, B. Tang, Catalase-like metal-organic framework nanoparticles to enhance radiotherapy in hypoxic cancer and prevent cancer recurrence, Chem. Sci. 10 (22) (2019) 5773–5778, https://doi.org/10.1039/c9sc00747d.
[29] F.R. Blattner, G. Plunkett 3rd, C.A. Bloch, N.T. Perna, V. Burland, M. Riley, J. Collado-Vides, J.D. Glasner, C.K. Rode, G.F. Mayhew, J. Gregor, N.W. Davis, H. A. Kirkpatrick, M.A. Goeden, D.J. Rose, B. Mau, Y. Shao, The complete genome sequence of Escherichia coli K-12, Science (New York, N.Y.) 277 (5331) (1997) 1453–1462, https://doi.org/10.1126/science.277.5331.1453.
[30] K.A. Datsenko, B.L. Wanner, One-step inactivation of chromosomal genes in Escherichia coli K-12 using PCR products, Proc. Natl. Acad. Sci. U. S. A 97 (12) (2000) 6640–6645, https://doi.org/10.1073/pnas.120163297.
[31] A.M. Feist, C.S. Henry, J.L. Reed, M. Krummenacker, A.R. Joyce, P.D. Karp, L. J. Broadbelt, V. Hatzimanikatis, B.Ø. Palsson, A genome-scale metabolic reconstruction for Escherichia coli K-12 MG1655 that accounts for 1260 ORFs and thermodynamic information, Mol. Syst. Biol. 3 (2007) 121, https://doi.org/10.1038/msb4100155.
[32] W. Zai, L. Kang, T. Dong, H. Wang, L. Yin, S. Gan, W. Lai, Y. Ding, Y. Hu, J.E. Wu, Coli membrane vesicles as a catalase carrier for long-term tumor hypoxia relief to enhance radiotherapy, ACS Nano 15 (9) (2021) 15381–15394, https://doi.org/10.1021/acsnano.1c07621.
[33] P. Riesz, T. Kondo, Free radical formation induced by ultrasound and its biological implications, Free Radic. Biol. Med. 13 (3) (1992) 247–270, https://doi.org/10.1016/0891-5849(92)90021-8.
[34] S.L. Herendeen, R.A. VanBogelen, F.C. Neidhardt, Levels of major proteins of Escherichia coli during growth at different temperatures, J. Bacteriol. 139 (1) (1979) 185–194, https://doi.org/10.1128/jb.139.1.185-194.1979.
[35] W.G. Pitt, S.A. Ross, Ultrasound increases the rate of bacterial cell growth, Biotechnol. Prog. 19 (3) (2003) 1038–1044, https://doi.org/10.1021/bp0340685.
[36] K.E. de Visser, J.A. Joyce, The evolving tumor microenvironment: from cancer initiation to metastatic outgrowth, Cancer Cell 41 (3) (2023) 374–403, https://doi.org/10.1016/j.ccell.2023.02.016.
[37] P. Stiefel, S. Schmidt-Emrich, K. Maniura-Weber, Q. Ren, Critical aspects of using bacterial cell viability assays with the fluorophores SYTO9 and propidium iodide, BMC Microbiol. 15 (2015) 36, https://doi.org/10.1186/s12866-015-0376-x.
[38] Q. Chen, J. Chen, C. Liang, L. Feng, Z. Dong, X. Song, G. Song, Z. Liu, Drug-induced co-assembly of albumin/catalase as smart nano-theranostics for deep intra-tumoral penetration, hypoxia relieve, and synergistic combination therapy, J. Contr. Release 263 (2017) 79–89, https://doi.org/10.1016/j.jconrel.2016.11.006.
[39] M.T. Duong, Y. Qin, S.H. You, J.J. Min, Bacteria-cancer interactions: bacteria-based cancer therapy, Exp. Mol. Med. 51 (12) (2019) 1–15, https://doi.org/10.1038/s12276-019-0297-0.
[40] C. Huang, F.B. Wang, L. Liu, W. Jiang, W. Liu, W. Ma, H. Zhao, Hypoxic tumor radiosensitization using engineered probiotics, Adv. Healthcare Mater. 10 (10) (2021), https://doi.org/10.1002/adhm.202002207.
[41] N.S. Forbes, Engineering the perfect (bacterial) cancer therapy, Nat. Rev. Cancer 10 (11) (Nov 2010) 785–794, https://doi.org/10.1038/nrc2934.
[42] M.R. Wu, B. Jusiak, T.K. Lu, Engineering advanced cancer therapies with synthetic biology, Nat. Rev. Cancer 19 (4) (Apr 2019) 187–195, https://doi.org/10.1038/s41568-019-0121-0.
[43] N.D. Taylor, A.S. Garruss, R. Moretti, S. Chan, M.A. Arbing, D. Cascio, J.K. Rogers, F.J. Isaacs, S. Kosuri, D. Baker, S. Fields, G.M. Church, S. Raman, Engineering an allosteric transcription factor to respond to new ligands, Nat. Methods 13 (2) (Feb 2016) 177–183, https://doi.org/10.1038/nmeth.3696.
[44] M. Lagator, C. Igler, A.B. Moreno, C.C. Guet, J.P. Bollback, Epistatic interactions in the arabinose cis-regulatory element, Mol. Biol. Evol. 33 (3) (Mar 2016) 761–769, https://doi.org/10.1093/molbev/msv269.
[45] S. Nuyts, L. Van Mellaert, J. Theys, W. Landuyt, P. Lambin, J. Anné, The use of radiation-induced bacterial promoters in anaerobic conditions: a means to control gene expression in clostridium-mediated therapy for cancer, Radiat. Res. 155 (5) (May 2001) 716–723, https://doi.org/10.1667/0033-7587(2001)155[0716:tuorib]2.0.co;2.
[46] J.X. Fan, Z.H. Li, X.H. Liu, D.W. Zheng, Y. Chen, X.Z. Zhang, Bacteria-mediated tumor therapy utilizing photothermally-controlled TNF-α expression via oral administration, Nano Lett. 18 (4) (Apr 11 2018) 2373–2380, https://doi.org/10.1021/acs.nanolett.7b05323.
[47] M.O. Din, T. Danino, A. Prindle, M. Skalak, J. Selimkhanov, K. Allen, E. Julio, E. Atolia, L.S. Tsimring, S.N. Bhatia, J. Hasty, Synchronized cycles of bacterial lysis for in vivo delivery, Nature 536 (7614) (Aug 4 2016) 81–85, https://doi.org/10.1038/nature18930.
[48] Y. Yang, Y. Wang, F. Zeng, Y. Chen, Z. Chen, F. Yan, Ultrasound-visible engineered bacteria for tumor chemo-immunotherapy, Cell Rep Med 5 (5) (2024), https://doi.org/10.1016/j.xcrm.2024.101512.
[49] P. Stiefel, S. Schmidt-Emrich, K. Maniura-Weber, Q. Ren, Critical aspects of using bacterial cell viability assays with the fluorophores SYTO9 and propidium iodide, BMC Microbiol. 15 (2015) 36, https://doi.org/10.1186/s12866-015-0376-x.